THE JOURNAL OF PHYSICAL CHEMISTRY Letters

pubs.acs.org/JPCL

Independence of Primary and Secondary Structures in Periodic Precipitation Patterns

Stoyan K. Smoukov, István Lagzi, and Bartosz A. Grzybowski*

Department of Chemical and Biological Engineering and Department of Chemistry, Northwestern University, 2145 Sheridan Road, Evanston, Illinois 60208, United States

ABSTRACT Microscopic periodic precipitation patterns featuring both primary and secondary bands form in thin gel films. The initial conditions for the precipitation process are defined by wet stamping and are chosen such that the primary and secondary structures are not necessarily collinear; the fact that these structures propagate in different directions suggests that they form independently of one another. This hypothesis is further supported by a theoretical model in which two different intermediate species mediate band formation.

SECTION Surfaces, Interfaces, Catalysis

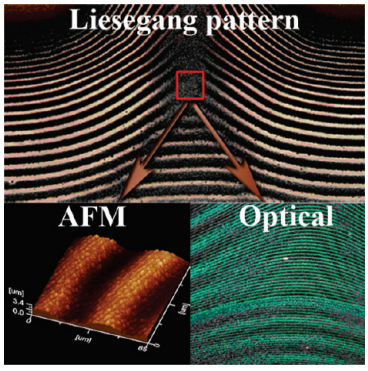

The study of periodic precipitation (PP) phenomena in general and the so-called Liesegang bands/rings (LR) in particular dates back to late 19th century.[1] The phenomenon occurs when two coprecipitating inorganic salts/electrolytes diffuse through certain gels,[2,3] rocks,[4−6] or even pathological human tissues.[7−10] For certain salt pairs,[11] the resulting precipitate is not uniformly distributed but forms discrete precipitation bands perpendicular to the direction of propagation of the invading (outer) electrolyte. Recently, there has been a resurgent interest in these reaction-diffusion phenomena, owing to their applications in bottom-up fabrication,[11] programmed assembly,[12] and symmetry breaking processes, with significant progress in controlling the locations of the bands, their sizes, spacing,[13,14] and even region-selective pattern formation.[14] Recent reports have examples of PP structures with submicrometer bands,[14] "reversed" (decreasing) band spacing,[15] helical patterns,[16,17] control of 3D topography,[14] dynamic control of pattern formation using electric fields[18−20] or light,[14] and rings made of oppositely charged nanoparticles.[21]

Developing mechanistic models describing these processes is crucial for improving our understanding and control of periodic precipitation phenomena at small scales and/or in constrained microgeometries.[22] Theoretical models of PP fall into two broad categories, prenucleation[23−26] and postnucleation ones.[27−30] In the first type, the nucleation and precipitation processes are not separated in space and time. These models assume that nucleation is spatially discontinuous and occurs only at the band-forming locations where the local concentration product of the electrolytes reaches some threshold value (governed by the solubility product of the forming precipitate). The nucleated particles grow, deplete electrolytes in their surroundings, and form an immobile precipitate, and the processes of diffusion, supersaturation, nucleation, and precipitation repeat form one band to another. The postnucleation models (e.g., competitive particle growth[27] or phase separation models)[30] do not require that nucleation and precipitation occur at the same location or time. Instead, the bands evolve through the nucleation of a mobile/diffusing precipitate, which grows by Ostwald ripening and ultimately aggregates into an immobile phase within the forming bands.

Both types of models reproduce the basic characteristics of PP patterns, although special modifications are often necessary to reproduce intricate details of the structures. One of the most prominent examples here are the so-called secondary structures, that is, microscopic bands superimposed onto the larger primary bands. No conclusive theoretical or experimental evidence has so far been provided to establish the relationship between these structures, and it is still unclear whether the secondary structures form independently of the primary bands. This limited understanding is largely due to the fact that experiments on the primary/secondary PP patterns have been typically conducted in long, cylindrical gel columns where the primary and secondary bands are always parallel due to the constant orientation of the "planar" front of the diffusing salts.

In this work, we propagate PP patterns in well-defined, two-dimensional microgeometries, in which the primary and the secondary bands are not necessarily collinear. Our experimental results and the accompanying theoretical model indicate that these two types of structures form independently of one another. Furthermore, the model suggests that primary bands form prior to the secondary ones.

Received Date: December 13, 2010
Accepted Date: January 14, 2011

DOI: 10.1021/jz101679t | *J. Phys. Chem. Lett.* **2011**, *2*, 345–349

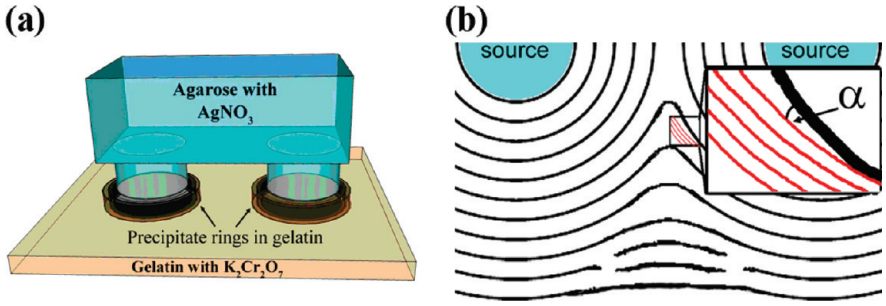

Figure 1. (a) Scheme of the experimental arrangement whereby the LRs are propagated in a ~20 μm thick $K_2Cr_2O_7$/gelatin film from circular features of an agarose stamp soaked with $AgNO_3$. (b) Top view of the developed LR pattern features both the thicker primary bands (colored black) and smaller secondary bands (only a fragment of the bands is shown in the boxed region). The primary and the secondary bands are not necessarily collinear, as illustrated by the α angle in the zoomed-in region.

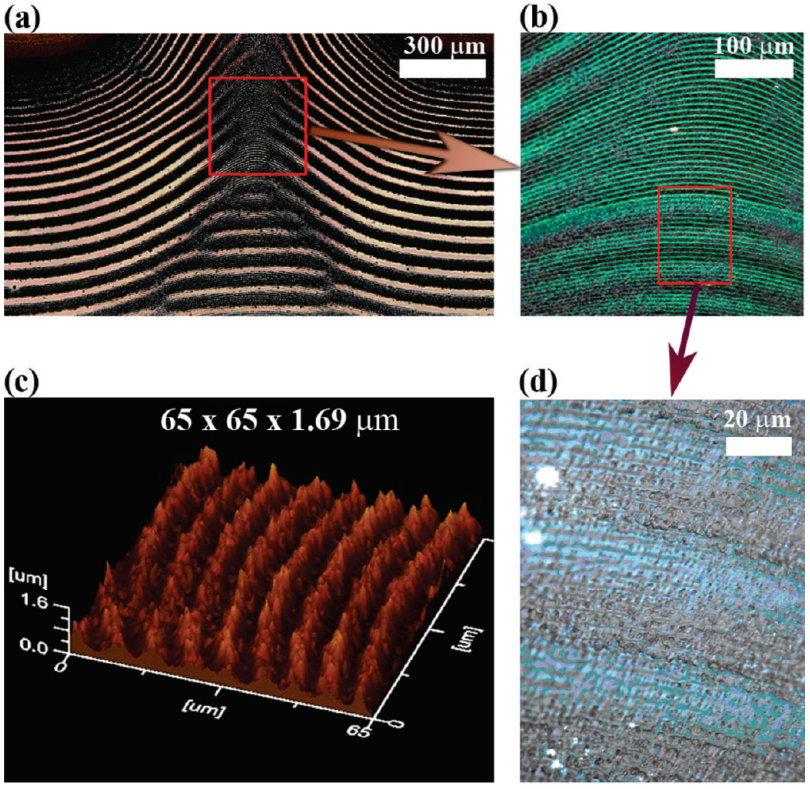

Figure 2. Experimental images of the LR patterns propagated from two nearby sources and featuring both primary and secondary bands. (a) A large-area optical image of the LRs. The secondary bands are clearly visible in (b) and are further magnified in the AFM scan in (c) (surface deformations correspond to LRs; see refs 13, 14, and 22 for details) and the optical image in (d). Note that in this particular region (relatively far away from the stamped features), the two types of bands are, to a good approximation, collinear.

Our experiments were based on the so-called wet stamping (WETS) technique,[11−13,31−35] in which an outer electrolyte (here, $AgNO_3$) is delivered from a hydrogel stamp micropatterned in bas-relief into a thin gel film doped with an inner electrolyte ($K_2Cr_2O_7$, Figure 1a)[13] Because the delivery of the outer electrolyte from the stamp is, to a good approximation, purely diffusive,[31] the sizes of the uniform (turbulent) precipitation zones around the stamped features are minimized,[13] allowing for the resolution of multiple micro- or even nanoscopic bands.[14] In addition, because the thin gel "buckles" proportionally to the amount of precipitate produced at a given location (see ref 13 for details), the bands can be studied not only by optical microscopy but also the atomic force microscopy (AFM), which reconstructs the topography of the buckled precipitation zones in fine detail.[14]

Here, we propagated the LRs from two nearby circular sources (Figure 1b). We hypothesized that because in this arrangement the shapes of the isoconcentration profiles and the direction of front propagation change with time, it might be possible to spatially "separate" the primary and the secondary bands such that they are not always collinear.[36] The stamps were made by casting a 10 % w/w solution of boiling

DOI: 10.1021/jz101679t | J. Phys. Chem. Lett. 2011, 2, 345–349

high-strength agarose (OmniPur, EM Science, Darmstadt, Germany) against lithographically defined polydimethylsiloxane (PDMS) masters presenting cylindrical depressions on their surfaces. After degassing and cooling for 30−60 min at room temperature, the agarose layer was gently peeled off from the PDMS master, cut into 1 cm ×1 cm × ∼0.5 cm square "stamps", and soaked in a 30 % w/w solution of $AgNO_3$ for 6−12 h. The gel films were made by spincoating a 2 in. × 3 in. glass slide with a gelatin solution containing the inner electrolyte potassium dichromate ($K_2Cr_2O_7$). The composition of this solution was 1.5 g of gelatin (Sigma, from bovine skin: Type B; gel strength: 225 Bloom), 0.3 g of $K_2Cr_2O_7$, 1.4 mL of ammonium hydroxide, and 20 mL of water. The slides were spin-coated at 300 rpm and left to dry in the dark overnight at room temperature. Prior to WETS, the gelatin layer was "strengthened" by irradiation with 0.7 mW/cm^2 of 254 nm UV light for 20 s, which caused additional cross-linking of the gel by Cr(III) ions.[14,35] Immediately prior to use, the stamps containing the outer electrolyte were dabbed onto a filter paper, had their surfaces blotted dry under a stream of nitrogen, and were placed on a clean Petri dish for 5 min (to equilibrate any hydration gradients that might have developed during drying). Subsequently, the stamps were applied onto the gel film to initiate pattern formation.

The fully developed LR patterns are shown in Figure 2. Both optical images (Figure 2a,b,d) of the rings as well as the AFM scans (Figure 2c) of surface buckling due to band formation reveal that these patterns exhibit both the primary and the secondary structures. The primary bands are ∼20 μm wide, 2−5 μm tall, and spaced by as much as 60 μm. The secondary bands, on the other hand, are ∼3−5 μm wide, 0.5−1 μm tall, and spaced by ∼5−8 μm. Importantly, although the two types of patterns are parallel near and far away from the two stamped features (cf. Figure 2a), they are not collinear (and even cross each other) in the regions between the sources, as illustrated in Figure 3. Moreover, the secondary structures are clearly visible in between the primary bands. In extreme cases, the secondary patterns are continuous across the fork defects of the primary bands (see Figure S1 in the Supporting Information, SI). Together, these observations suggest that secondary structures do not form by simple redistribution of particles within the primary bands and that the mechanism of their formation is likely independent of that of primary structures. In this context, we note that recent experiments on LR in the $AgNO_3/Ag_2Cr_2O_7$/gelatin system conducted by one of the authors (I.L., see ref 37) indicate that secondary bands form after the nearby primary rings have developed (see ref 38 for a movie illustrating this process).

To rationalize our experimental observations, we developed a theoretical model based on the Cahn−Hilliard equation,[30,39,40] which is a powerful tool for describing phase separation and precipitation phenomena and, when combined with reaction-diffusion, can reproduce periodic precipitation in both the "classical" LR cases and also systems involving electric fields or 3D patterns.[37,41] In our case, patterns comprising primary/secondary structures can be reproduced if, in the CH formalism, we assume that the primary and the secondary bands consist of two different types of intermediates/precipitates forming at different time scales,[42] and these precipitation processes (primary and secondary) are separated kinetically and thermodynamically Thus, the free energy is approximated as a sum of the free energies of the two precipitates, and the functional forms of these free energies are assumed to be the same, $F_1(x) = F_2(x) = f(x)$. While the nature of these intermediates cannot be verified experimentally, one plausible interpretation would be that they contain different types of precipitates (either in terms of the size or compositions of the precipitate's particles).

In our model, the outer electrolyte, A, diffuses from an agarose stamp into the gelatin layer and reacts with the inner electrolyte, B, to give an intermediate sol species C_1, $A + B \xrightarrow{k} C_1$. This sol can diffuse and phase separate until ultimately forming an immobile precipitate C, $C_1 \xrightarrow{\kappa_1} C$. In addition, intermediate C_1 can transform into another intermediate D_1, which can diffuse and phase separate before transforming into an immobile precipitate D, $C_1 \xrightarrow{\kappa_2} D_1 \xrightarrow{\kappa_3} D$. Combining these reactions with the diffusion of the species involved, the equations governing the dynamics of the system take the following form:

$$\partial_t a = D\Delta a - kab \tag{1}$$

$$\partial_t b = D\Delta b - kab \tag{2}$$

$$\partial_t c_1 = D_1\Delta c_1 + kab - \kappa_1 c_1 - \kappa_2 c_1 \tag{3}$$

$$\partial_t c = -\lambda_c\Delta\left(\frac{\delta f}{\delta c}\right) + \kappa_1 c_1 \tag{4}$$

$$\partial_t d_1 = D_1\Delta d_1 + \kappa_2 c_1 - \kappa_3 d_1 \tag{5}$$

$$\partial_t d = -\lambda_d\Delta\left(\frac{\delta f}{\delta d}\right) + \kappa_3 d_1 \tag{6}$$

Here a, b, c_1, c, d_1, and d are the concentrations of the appropriate species, f is the free energy of the system, Δ is the Laplace operator, and parameters λ determine the time scales of phase separation. D is the diffusion coefficient of the A and B, D_1 is the diffusion coefficient of the intermediate species C_1 and D_1 (we assume that the intermediate species diffuse slower than either the inner or the outer electrolytes), while k, κ_1, κ_2, and κ_3 are the chemical reaction rate constants, as defined previously. We take k to be large, resulting in a reaction zone of negligible width (this assumption is compatible with the observations in typical LR experiments). In eqs 4 and 6, the free energy of the system is assumed to have minima at some low (c_{low}) and high (c_{high}) concentrations, and it is assumed to be of a Ginzburg−Landau form.[30,40] Its functional derivative is most compactly given in terms of a shifted and rescaled concentration $m = (2c - c_{high} - c_{low})/(c_{high} - c_{low})$

$$\frac{c_h - c_1}{2}\frac{\delta f}{\delta c} = \frac{\delta f}{\delta m} = m - m^3 + \sigma\Delta m \tag{7}$$

Similar transformation can be applied to d. Parameters λ in eqs 4 and 6 and σ in eq 7 are setting the spatial and the time scales, respectively. In eqs 4 and 6, $\lambda_c \neq \lambda_d$ to ensure the time

DOI: 10.1021/jz101679t | J. Phys. Chem. Lett. 2011, 2, 345–349

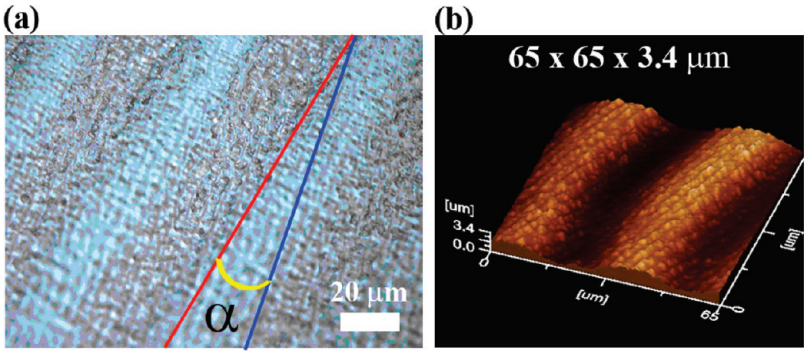

Figure 3. Close to and in between the stamped features, the primary and the secondary structures are not collinear, as indicated by the angle α. Here, the smaller secondary bands "cross over" the larger primary "waves"; (a) an optical micrograph; (b) the AFM scan of the surface, whereby surface deformations coincide with the locations of the deposited precipitate.

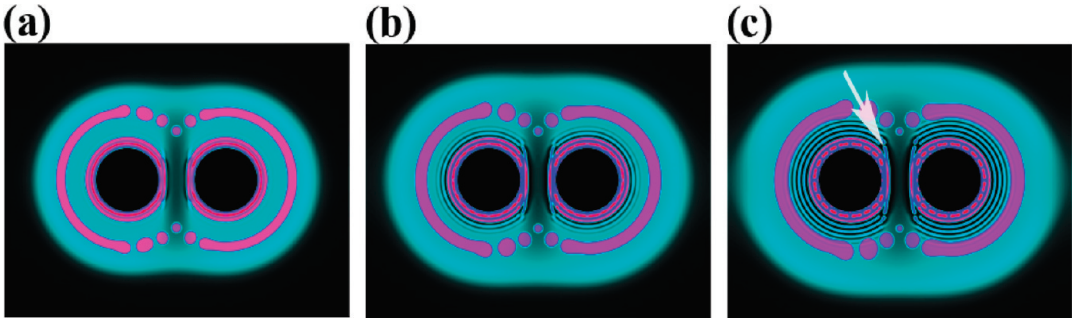

Figure 4. Modeled primary (pink) and secondary (green or red if within primary bands) patterns in a 2D Liesegang system at times $t = 300$ (a), 400 (b), and 500 (c). Note that primary bands form first. The simulation used the following parameter set: $D = 1, D_1 = 0.1, D = 1, \lambda_c = 1, \lambda_d = 0.025, \sigma = 1, k = 0.1, \kappa_1 = 0.01, \kappa_2 = 0.01$, and $\kappa_3 = 0.1$. The size of the domain is 700 × 700. The grid spacing and the time step are 1.0 and 0.02, respectively.

scale separation in precipitation processes. In a typical simulation, the values of parameters producing both primary and secondary bands were $D = 1, D_1 = 0.1, \lambda_c = 1, \lambda_d = 0.025, \sigma = 1, k = 0.1, \kappa_1 = 0.01, \kappa_2 = 0.01$, and $\kappa_3 = 0.1$. Partial differential eqs 1−6 were discretized on a uniform square grid and were solved using a backward Euler method. The initial conditions were set to match the experiments. The inner electrolyte was homogeneously distributed in the gelatin domain with concentration b_0, while the initial concentrations for the other species were set to 0. The outer electrolyte diffused from outside with the fixed concentration at the boundary ($a(t,x) = a_0$). No-flux boundary conditions were applied at the boundaries of the gelatin domain.

Figure 4 illustrates that the model reproduces the main experimental observations and can capture independent spatiotemporal formation of the primary and secondary bands. Specifically, primarily bands are predicted to form first followed by the formation of secondary bands; while this conclusion cannot be directly verified in the micropatterns studied here, it agrees with our previous experiments described in ref 37. Also, our model confirms that the secondary bands form not only in between the primary ones, but the two types of structures can also coexist in the same locations (i.e., secondary bands are superimposed onto the primary ones; cf. Figure 4 versus Figure 3) and are not necessarily parallel to one another (e.g., region marked with an arrow in Figure 4c). On the other hand, we note that the Cahn−Hillard equation cannot reproduce continuous bands in the regions directly between the circular sources, where the curvature of continuous rings would be high. Consequently, in an effort to minimize free energy, the CH equation separates the bands into energetically more favorable circular regions. We note that the inability to deal with highly curved patterns is a well-known limitation of the CH approach.

In summary, the major finding of our study is that secondary structures in Liesegang patterns develop independently of the primary ones, likely on different time scales. The model that we developed can be used to guide rational design of complex primary/secondary band structures for potential uses as nonbinary optical gratings.[11,13,14] In a wider context, we suggest that the WETS method of propagating PP patterns from low-symmetry microgeometries, where the concentration gradients change direction in time, can become a useful method for spatially resolving pattern-forming processes characterized by a temporal offset.

SUPPORTING INFORMATION AVAILABLE Additional experimental images. This material is available free of charge via the Internet at http://pubs.acs.org.

DOI: 10.1021/jz101679t | J. Phys. Chem. Lett. 2011, 2, 345–349

AUTHOR INFORMATION

Corresponding Author:

*To whom correspondence should be addressed. E-mail: grzybor@northwestern.edu.

ACKNOWLEDGMENT The authors thank Dr. Marcin Fialkowski and Dr. Agnieszka Bitner for their help in the early stages of the project. This work was supported by the Nonequilibrium Energy Research Center, which is an Energy Frontier Research Center funded by the U.S. Department of Energy, Office of Science, Office of Basic Energy Sciences under Award DESC0000989.

REFERENCES

(1) Liesegang, R. E. Uber Einige Eigenschaften von Gallerten. *Naturwiss. Wochenschr.* **1896,** *11*, 353–362.
(2) Henisch, H. K. Liesegang Ring Formation in Gels. *J. Cryst. Growth* **1986,** *76*, 279–289.
(3) Müller, S. C.; Ross, J. Spatial Structure Formation in Precipitation Reactions. *J. Phys. Chem. A* **2003,** *107*, 7997–8008.
(4) Allegre, C. J.; Provost, A.; Jaupart, C. Oscillatory Zoning — A Pathological Case of Crystal Growth. *Nature* **1981,** *294*, 223–228.
(5) Haase, C. S.; Chadam, J.; Feinn, D.; Ortoleva, P. Oscillatory Zoning in Plagioclase Feldspar. *Science* **1980,** *209*, 272–274.
(6) Ortoleva, P. J. *Geochemical Self-Organization*; Oxford University Press: New York, 1994.
(7) Glazier, D. B.; Murphy, D. P.; Cummings, K. B.; Morrow, F. A. Liesegang Rings. *J. Urol.* **1997,** *157*, 940–941.
(8) Perrotta, P. L.; Ginsburg, F. W.; Siderides, C. I.; Parkash, V. Liesegang Rings and Endometriosis. *Int. J. Gynecol. Pathol.* **1998,** *17*, 358–362.
(9) Misselevich, I.; Boss, J. H. Liesegang Rings in a Giant Proliferating Trichilemmal Tumor. *Int. J. Dermatol.* **1999,** *38*, 954–955.
(10) Gilchrist, H. M.; Wick, M. R.; Patterson, J. W. Liesegang Rings in an Apocrine Hidrocystoma: a Case Report and Review of Literature. *J. Cutan. Pathol.* **2010,** *37*, 1064–1066.
(11) Grzybowski, B. A.; Bishop, K. J. M.; Campbell, C. J.; Fialkowski, M.; Smoukov, S. K. Micro- and Nanotechnology via Reaction-Diffusion. *Soft Matter* **2005,** *1*, 114–128.
(12) Grzybowski, B. A.; Campbell, C. J. Fabrication with 'Programmable' Chemical Reactions. *Mater. Today* **2007,** *10*, 38–46.
(13) Bensemann, I. T.; Fialkowski, M.; Grzybowski, B. A. Wet Stamping of Microscale Periodic Precipitation Patterns. *J. Phys. Chem. B* **2005,** *109*, 2774–2778.
(14) Smoukov, S. K.; Bitner, A.; Campbell, C. J.; Kandere-Grzybowska, K.; Grzybowski, B. A. Nano- and Microscopic Surface Wrinkles of Linearly Increasing Heights Prepared by Periodic Precipitation. *J. Am. Chem. Soc.* **2005,** *127*, 17803–17807.
(15) Molnár, F.; Izsák, F.; Lagzi, I. Design of Equidistant and Revert Type Precipitation Patterns in Reaction-Diffusion Systems. *Phys. Chem. Chem. Phys.* **2008,** *10*, 2368–2373.
(16) Müller, S. C.; Kai, S.; Ross, J. Curiosities in Periodic Precipitation Patterns. *Science* **1982,** *216*, 635–637.
(17) Suganthi, R. V.; Girija, E. K.; Kalkura, S. N.; Varma, H. K.; Rajaram, A. Self-Assembled Right Handed Helical Ribbons of the Bone Mineral Hydroxyapatite. *J. Mater. Sci.: Mater. Med.* **2009,** *20*, 131–136.
(18) Al-Ghoul, M.; Sultan, R. Front Propagation in Patterned Precipitation. II. Electric Effects in Precipitation-Dissolution Patterning Schemes. *J. Phys. Chem. A* **2003,** *107*, 1095–1101.
(19) Bena, I.; Droz, M.; Rácz, Z. Formation of Liesegang Patterns in the Presence of an Electric Field. *J. Chem. Phys.* **2005,** *122*, 204502.
(20) Lagzi, I. Formation of Liesegang Patterns in an Electric Field. *Phys. Chem. Chem. Phys.* **2002,** *4*, 1268–1270.
(21) Lagzi, I.; Kowalczyk, B; Grzybowski, B. A. Liesegang Rings Engineered from Charged Nanoparticles. *J. Am. Chem. Soc.* **2010,** *132*, 58–60.
(22) Grzybowski, B. A. *Chemistry in Motion: Reaction-Diffusion Systems for Micro- and Nanotechnology*; Wiley: Chichester, U. K., 2009.
(23) Ostwald, W. Zur Theorie der Liesegang'schen Ringe. *Kolloid Z.* **1925,** *36*, 380–390.
(24) Wagner, C. Mathematical Analysis of the Formation of Periodic Precipitations. *J. Colloid Sci.* **1950,** *5*, 85–97.
(25) Prager, S. Periodic Precipitation. *J. Chem. Phys.* **1956,** *25*, 279–283.
(26) Keller, J. B.; Rubinow, S. I. Recurrent Precipitation and Liesegang Rings. *J. Chem. Phys.* **1981,** *74*, 5000–5007.
(27) Feeney, R.; Schmidt, S. L.; Strickholm, P.; Chandam, J.; Ortoleva, P. Periodic Precipitation and Coarsening Waves: Applications of the Competitive Particle Growth Model. *J. Chem. Phys.* **1983,** *78*, 1293–1311.
(28) Venzl, G. Pattern Formation in Precipitation Processes. I. The Theory of Competitive Coarsening. *J. Chem. Phys.* **1986,** *85*, 1996–2005.
(29) Venzl, G. Pattern Formation in Precipitation Processes. II. A Postnucleation Theory of Liesegang Bands. *J. Chem. Phys.* **1986,** *85*, 2006–2011.
(30) Rácz, Z. Formation of Liesegang Patterns. *Physica A* **1999,** *274*, 50–59.
(31) Fialkowski, M.; Campbell, C. J.; Bensemann, I. T.; Grzybowski, B. A. Absorption of Water by Thin, Ionic Films of Gelatin. *Langmuir* **2004,** *20*, 3513–3516.
(32) Klajn, R.; Fialkowski, M.; Bensemann, I. T.; Bitner, A.; Campbell, C. J.; Bishop, K.; Smoukov, S.; Grzybowski, B. A. Multicolour Micropatterning of Thin Films of Dry Gelatin. *Nat. Mater.* **2004,** *3*, 729–735.
(33) Campbell, C. J.; Fialkowski, M.; Klajn, R.; Bensemann, I. T.; Grzybowski, B. A. Color Micro- and Nanopatterning with Counter-Propagating Reaction-Diffusion Fronts. *Adv. Mater.* **2004,** *16*, 1912–1917.
(34) Campbell, C. J.; Baker, E.; Fialkowski, M.; Grzybowski, B. A. Arrays of Microlenses of Complex Shapes Prepared by Reaction-Diffusion in Thin Films of Ionically Doped Gels. *Appl. Phys. Lett.* **2004,** *85*, 1871–1873.
(35) Paszewski, M.; Smoukov, S. K.; Klajn, R.; Grzybowski, B. A. Multilevel Surface Nanostructuring via Sequential Photoswelling of Dichromated Gelatin. *Langmuir* **2007,** *23*, 5419–5422.
(36) Note that with more symmetric geometries, this would not be true because both types of structures would always be parallel (e.g., concentric for a circular source).
(37) Bena, I.; Droz, M.; Lagzi, I.; Martens, K.; Rácz, Z.; Volford, A. Designed Patterns: Flexible Control of Precipitation Through Electric Currents. *Phys. Rev. Lett.* **2008,** *101*, 075701.
(38) http://nimbus.elte.hu/~lagzi/tau_300s.mpg.
(39) Cahn, J. W.; Hilliard, J. E. Free Energy of a Non-Uniform System I: Interfacial Energy. *J. Chem. Phys.* **1958,** *28*, 258–266.
(40) Antal, T.; Droz, M.; Magnin, J.; Rácz, Z. Formation of Liesegang Patterns: A Spinodal Decomposition Scenario. *Phys. Rev. Lett.* **1999,** *83*, 2880–2883.
(41) Volford, A.; Lagzi, I.; Molnár, F., jr.; Rácz, Z. Coarsening of Precipitation Patterns in a Moving Reaction-Diffusion Front. *Phys. Rev. E* **2009,** *80*, 055102(R).
(42) George, J.; Varghese, G. Migrating Triplet Precipitation Bands of Calcium Phosphates in Gelatinous Matrix. *J. Mater. Sci.* **2005,** *40*, 5557–5559.

DOI: 10.1021/jz101679t | *J. Phys. Chem. Lett.* **2011,** *2*, 345–349